Vacancies and small polarons in $SrTiO_3$

Anderson Janotti, Joel B. Varley,* Minseok Choi,† and Chris G. Van de Walle
Materials Department, University of California, Santa Barbara, California 93106-5050, USA
(Received 28 April 2014; revised manuscript received 15 July 2014; published 18 August 2014)

Using first-principles calculations we investigate the impact of intrinsic defects and small polarons on the electrical and optical properties of $SrTiO_3$. We pay special attention to the seemingly contradictory role of oxygen vacancies as shallow donor and source of deep-level luminescence, as reported in the literature. We find that oxygen vacancies are double donors, and that one electron is easily ionized, explaining the shallow donor behavior. The second electron is trapped in the form of a small polaron, and this additional binding energy explains the behavior as a deep center that gives rise to blue luminescence. At low temperatures, holes become self-trapped, and recombination of free electrons with self-trapped holes gives rise to green luminescence. These results explain the intricate interplay between the observed green and blue luminescence in $SrTiO_3$, and form a framework for interpreting similar phenomena in other complex oxides.

DOI: 10.1103/PhysRevB.90.085202 PACS number(s): 71.55.−i, 61.72.Bb

I. INTRODUCTION

$SrTiO_3$ (STO) crystallizes in the perovskite structure, has a wide band gap of 3.25 eV [1], and it is often regarded as a prototype complex oxide. It has served as a substrate to grow other oxides, and it forms the basis for the complex-oxide heterostructures that display two-dimensional electron gases [2,3]. Experiments indicate that defects such as oxygen vacancies easily form and strongly affect the electrical and optical properties, simultaneously acting as a shallow donor and as a deep center that causes luminescence well below the band-gap energy. Oxygen vacancies have been invoked as a source of *n*-type conductivity, which has been observed to vary with oxygen partial pressure in the growth or annealing environment [4–8]. Annealing under oxygen-rich conditions suppresses the conductivity, while annealing in vacuum leads to an increase in conductivity. This effect has been interpreted in terms of annihilation or formation of oxygen vacancies [4–7], which are thus implicitly assumed to behave as shallow donors, i.e., point defects with electronic levels very close to the conduction band. On the other hand, a strong and broad blue luminescence peak (2.8–2.9 eV), typically observed at room temperature in STO that has been irradiated, or annealed in vacuum, has also been attributed to oxygen vacancies [6–8]. It seems contradictory that the oxygen vacancy could simultaneously be a shallow donor contributing to *n*-type conductivity *and* be a source of deep-level luminescence—i.e., emit photons with energies significantly lower than the band gap.

Several groups have investigated the luminescence spectrum of STO through photoluminescence (PL) [6,7,9–14] or cathodoluminescence (CL) [8,15–17] experiments, and conflicting interpretations have been put forward to explain the observed peaks. At temperatures below 100 K, the luminescence spectrum of STO is typically dominated by a broad green luminescence band peaking at 2.4–2.5 eV [6,7,9–14]. At higher temperatures, the green band decreases, and is replaced by a broad peak in the blue (2.8–2.9 eV) [6,7,9,14]. Some authors have proposed that the green band is caused by a recombination of a self-trapped exciton, in which the electron and hole are localized on neighboring Ti and O atoms [10,11,18]. Others have attributed the green luminescence to the radiative decay of an exciton bound to an oxygen-related defect [6] or to other unknown structural intrinsic defects [13]. The blue luminescence, on the other hand, has been associated with oxygen vacancies [6,7], or with recombination of a free electron with a localized self-trapped hole [12]. The mechanism behind the spectral change from low to high temperatures, in which the intensity of the green luminescence decreases and the blue peak emerges, has also remained unresolved. A model based on single-carrier trapping, bimolecular recombination, and Auger recombination was proposed [9], but did not address the microscopic origins of the luminescence.

First-principles electronic structure calculations for defects in STO have also been reported [19–23], most of them focusing on the oxygen vacancy. The issue of what is the most stable charge state of the vacancy in *n*-type STO is still being debated, even among research groups using similar methods [22,23]. Lin *et al.* [22] reported that the oxygen vacancy is stable in the neutral charge state if the Fermi level is more than 2.6 eV above the valence band; Choi *et al.* [23], on the other hand, concluded that the vacancy is stable in a singly positive charge state when the Fermi level is at the conduction-band minimum.

In the present work we untangle these puzzling results, using first-principles calculations based on density functional theory with a screened hybrid functional. We find that the oxygen vacancy is a double donor in which the two electrons display very different behavior: one electron is easily ionized, explaining the shallow-donor character. The other is self-trapped near the vacancy in the form of a small polaron; it is this electron state that gives rise to the deep-level behavior and the below-gap blue luminescence.

II. COMPUTATIONAL METHOD

The calculations are based on the generalized Kohn-Sham theory [24] with the screened hybrid functional of

*Present address: Lawrence Livermore National Laboratory, Livermore, CA 94550 USA.
†Present address: Korea Institute of Materials Science, Changwon 642-831, Republic of Korea.

Heyd, Scuseria, and Ernzerhof (HSE) [25]. The interactions between the valence electrons and the ionic cores are treated using projector augmented wave (PAW) potentials [26] as implemented in the VASP code [27]. The PAW potentials for Sr, Ti, and O contain 10, 4, and 6 valence electrons, respectively, i.e., Sr:$4s^2 4p^6 5s^2$, Ti:$4s^2 3d^2$, and O:$2s^2 2p^4$. The calculated lattice parameter of 3.913 Å for the cubic phase of STO is in good agreement with the experimental value of 3.905 Å [28], as are the calculated indirect (R-Γ, 3.20 eV; expt.: 3.25 eV) and direct (Γ-Γ, 3.58 eV; expt.: 3.70 eV) band gaps [1]. The defects and small polarons were simulated using a supercell of 135 atoms, which is a $3 \times 3 \times 3$ repetition of the five-atom primitive cell of cubic STO. A $2 \times 2 \times 2$ mesh of special k points is used for integrations over the Brillouin zone and a cutoff of 400 eV is used for the plane-wave basis set. We derive thermodynamic transition levels from the formation energies for each defect in all possible charge states, and determine optical emission energies from formation-energy differences.

The formation energy of a vacancy V_X (X = Sr, Ti, O) in charge state q is given by

$$E^f\left(V_X^q\right) = E_{\text{tot}}\left(V_X^q\right) - E_{\text{tot}}(\text{STO}) + \mu_X + q \cdot E_{\text{F}} + \Delta^q, \tag{1}$$

where $E_{\text{tot}}(V_X^q)$ is the total energy of the supercell containing a vacancy of the species X in charge state q and E_{tot}(STO) is the total energy of an STO perfect crystal in the same supercell. The atom of species X that is removed from the crystal is placed in a reservoir of energy μ_X, referenced to the total energy per atom of the standard phase for the element X. The Fermi level E_{F} is the energy of the electron reservoir in the solid, referenced to the valence-band maximum of the STO perfect crystal. The last term Δ^q is a charge-state dependent correction due to the finite size of the supercell [29,30].

The chemical potentials μ_X (X = Sr, Ti, O) are treated as variables, and can be chosen to represent experimental conditions. They must satisfy the stability condition of STO, namely,

$$\mu_{\text{Sr}} + \mu_{\text{Ti}} + 3\mu_{\text{O}} = \Delta H_f(\text{STO}), \tag{2}$$

where ΔH_f(STO) is the formation enthalpy of STO. The chemical potentials are also bound by the formation of limiting phases such as TiO_2 and SrO:

$$\mu_{\text{Ti}} + 2\mu_{\text{O}} \leqslant \Delta H_f(\text{TiO}_2), \tag{3}$$

$$\mu_{\text{Sr}} + \mu_{\text{O}} \leqslant \Delta H_f(\text{SrO}), \tag{4}$$

where $\Delta H_f(TiO_2)$ and ΔH_f(SrO) are the formation enthalpies of rutile TiO_2 and SrO in the rocksalt crystal structure. The calculated formation enthalpies $\Delta H_f(\text{STO}) = -16.7$ eV, $\Delta H_f(TiO_2) = -9.7$ eV, and $\Delta H_f(\text{SrO}) = -5.8$ eV are in good agreement with the experimental values [31].

The chemical potential μ_{O} can in principle vary over a wide range, from $\mu_{\text{O}} = 0$ to $\mu_{\text{O}} = 1/3\Delta H_f(\text{STO}) = -5.6$ eV. For a given μ_{O}, μ_{Ti} can vary from $\mu_{\text{Ti}} = \Delta H_f(TiO_2) - 2\mu_{\text{O}}$ to $\mu_{\text{Ti}} = \Delta H_f(\text{STO}) - \Delta H_f(\text{SrO}) - 2\mu_{\text{O}}$; the corresponding limits on μ_{Sr} are $\mu_{\text{Sr}} = \Delta H_f(\text{STO}) - \Delta H_f(TiO_2) - \mu_{\text{O}}$ and $\mu_{\text{Sr}} = \Delta H_f(\text{SrO}) - \mu_{\text{O}}$, respectively. Here, we present results for $\mu_{\text{O}} = -3.1$ eV, corresponding to equilibrium with an O_2 gas at $T = 1000\,^{\circ}$C and $p_{O_2} = 2 \times 10^{-11}$ Torr [32] to represent vacuum annealing. We also set $\mu_{\text{Ti}} = -4.0$ eV and $\mu_{\text{Sr}} = -3.4$ eV, by taking TiO_2 as a limiting phase. Formation energies for other conditions can be obtained by using Eqs. (1)–(4).

III. RESULTS AND DISCUSSION

A. Oxygen vacancy

Each oxygen atom in STO is bonded to two Ti atoms. Therefore, forming an oxygen vacancy (V_{O}) results in two Ti dangling bonds, which combine into bonding and antibonding states. These states are composed mostly of d_{z^2}, which forms the σ bond between Ti and O. In the neutral charge state, V_{O}^0, the bonding state is 0.15 eV below the conduction band and occupied with two electrons of opposite spins. The two Ti atoms are slightly displaced towards the vacancy, by 1.4% of the equilibrium Ti-O bond length as illustrated in Fig. 1(a). In the singly positive charge state, V_{O}^+, the bonding state is occupied by one electron, making the center paramagnetic with $S = 1/2$; the occupied spin-up bonding state is 0.51 eV below the conduction band and the spin-down state is resonant in the conduction band. The two Ti atoms are displaced away from the vacancy by 3.1%, and the spin density is mostly located in the vacant site, as shown in Fig. 1(b). Similar results for the single-particle states of V_{O}^0 and V_{O}^+ were obtained by Alexandrov *et al.*, using a hybrid functional based on a localized basis set [21]. The doubly positive charge state, V_{O}^{+2}, is characterized by large outward displacements of the Ti atoms, by 6.7% [Fig. 1(c)]; in this case, both bonding and antibonding states are unoccupied and lie as resonances in the conduction band.

We also find that V_{O}^{+2} can trap up to two electrons in the form of small polarons, in which the electrons are localized on individual Ti atoms near the vacancy [Figs. 1(d)–1(f)], turning

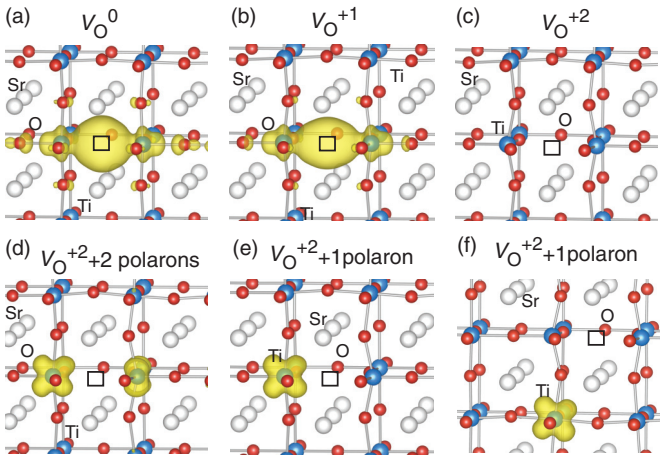

FIG. 1. (Color online) Oxygen vacancy in $SrTiO_3$ in different charge states. (a) Neutral V_{O}^0. (b) Singly positive V_{O}^{+1}. (c) Doubly positive V_{O}^{+2}. The complexes of V_{O}^{+2} with small polarons are also shown: (d) the charge neutral complex (V_{O}^{+2}+ 2 polarons) and (e),(f) two different configurations of the singly positive complex (V_{O}^{+2}+ 1 polaron). The vacancy location is indicated with an empty square. The isosurfaces correspond to 10% of the maximum value in each plot.

their oxidation state to Ti^{3+}. The complex of a V_O^{+2} with two polarons, shown in Fig. 1(d), is overall charge neutral, but it is clearly distinguished from the V_O^0 in Fig. 1(a): in V_O^0, the trapped electrons are localized within the vacancy and occupy defect states in the band gap, while in the complex the electrons are trapped in the form of polarons, localized on Ti atoms near the vacancy, which itself is in a +2 charge state and has no defect states in the band gap. A complex can also be formed between V_O^{+2} and one small polaron, as shown in Figs. 1(e) and 1(f), effectively acting as a single donor. The lowest energy configuration is shown in Fig. 1(f). We note that the polarons next to the vacancy do not show a d_{z^2} character, indicating that they do not originate from the broken Ti-O σ bond of the oxygen vacancy. Instead, they exhibit d_{xy}, d_{yz}, or d_{zx} character, associated with the e_g states that form the bottom of the STO conduction band.

These results clearly indicate that small electron polarons tend to form near the oxygen vacancy, raising the question of whether small polarons also exist as isolated species in STO. To answer this question, we studied the possible formation of a self-trapped electron in STO, in the absence of any vacancy, by adding an electron to a stoichiometric supercell, breaking the local symmetry around a given Ti atom and allowing the lattice to relax. We find that the excess electron indeed becomes localized on one Ti atom, leading to an expansion of the Ti-O bond length by 2.3% [see Fig. 2(a)]. However, the total energy of the supercell containing the isolated small polaron is 0.12 eV higher in energy than having an electron delocalized at the bottom of the conduction band. This is in contrast to what was found in TiO_2, where an isolated small polaron is lower in energy than a delocalized electron in the conduction band [33]. Therefore, we conclude that excess electrons in bulk STO do not become localized in the form of small polarons, but may materialize in the presence of a defect such as the oxygen vacancy.

We also note that the complex formed of V_O^{+2} and two polarons can assume a number of different configurations in which the polarons are localized on different Ti atoms around the vacancy, including Ti atoms that are not nearest neighbors of the vacancy. All these configurations result in total energies that differ by less than 0.33 eV, which represents the energy gain when removing one polaron from the complex. Similarly, the complex of V_O^{+2} and one polaron can assume different configurations where the trapped polaron can occupy different

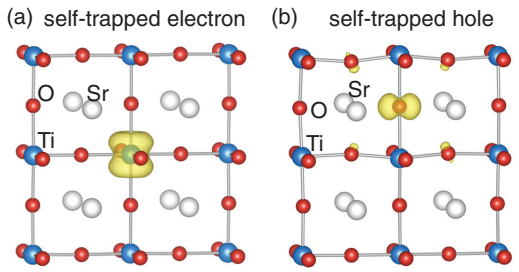

FIG. 2. (Color online) Spin density of self-trapped carriers in $SrTiO_3$. (a) Self-trapped electron. (b) Self-trapped hole. The isosurfaces correspond to 10% of the maximum value in each plot.

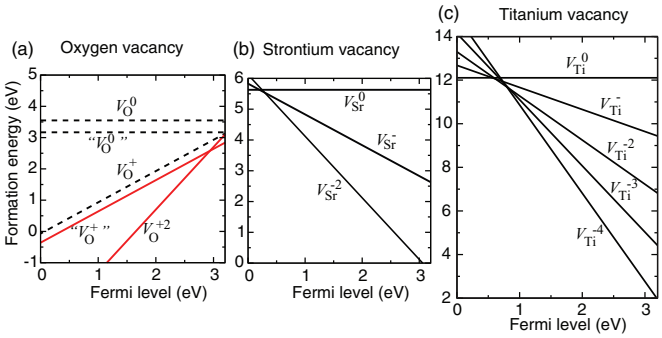

FIG. 3. (Color online) Formation energy as a function of Fermi level for vacancy defects in $SrTiO_3$. (a) Oxygen vacancy. The formation energies for the complexes with one and two polarons are also shown. (b) Sr vacancy. (c) Ti vacancy.

Ti atoms around the vacancy [two of which are shown in Figs. 1(e) and 1(f)]. These configurations vary in a range limited by the energy required to remove the polaron from the vacancy, which is 0.26 eV. This quantity can also be interpreted as the binding energy of the complex.

The formation energy of the oxygen vacancy as a function of the Fermi-level position is shown in Fig. 3(a). The neutral V_O^0 and singly ionized V_O^{+1} configurations are always higher in energy than the doubly ionized charge state V_O^{+2}, even in n-type STO in which the Fermi level lies near the bottom of the conduction band. This indicates that the oxygen vacancy is a double donor. The formation energies of the complexes between V_O^{+2} and one or two polarons are also shown in Fig. 3(a). The complex formed of V_O^{+2} and one polaron turns out to be the most stable configuration for Fermi levels near the conduction band. V_O^{+2} with two polarons, on the other hand, is always higher in energy. Our results, therefore, show that in n-type STO each oxygen vacancy traps one small polaron, remaining in a +1 charge state and contributing one electron to the conduction band.

B. Strontium and titanium vacancies

Due to the ionic nature of the bond between the Sr atoms and the TiO_6 octahedra in STO, the Sr vacancy does not lead to dangling bonds. Instead, in the neutral charge state, the Sr vacancy leaves two holes in the valence band, which is derived mostly from O $2p$ states. The holes, in turn, prefer to become localized on separate O atoms next to the vacancy, forming hole polarons. In Fig. 4(a) we show the spin density of the neutral Sr vacancy. The holes prefer to occupy O sites next to the vacancy, but stay as far as possible away from each other in order to minimize Coulomb repulsion. As in the case of small electron polarons near a doubly ionized oxygen vacancy, configurations in which the holes occupy different O sites near the Sr vacancy differ in energy by less than 0.20 eV.

The Sr vacancy can also be stabilized in the singly negative V_{Sr}^{-1} [Fig. 4(b)] and doubly negative V_{Sr}^{-2} [Fig. 4(c)] charge states. Formation energies for the different charge states are shown in Fig. 3(b). The Sr vacancy is a double acceptor, acting as a compensation center in n-type STO. The transition levels

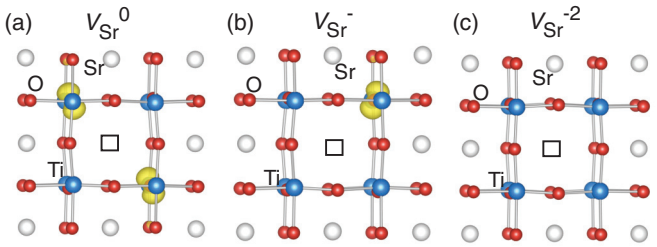

FIG. 4. (Color online) Strontium vacancy in $SrTiO_3$ in different charge states. (a) Neutral V_{Sr}^{0}. (b) Singly negative V_{Sr}^{-}. (c) Doubly negative V_{Sr}^{-2}. The vacancy location is indicated with an empty square. The spin densities for V_{Sr}^{0} and V_{Sr}^{-} are also shown, with the isosurfaces corresponding to 10% of the maximum.

from–2 to –1 and from –1 to neutral occur at 0.30 eV and 0.20 eV above the valence band.

The removal of a Ti atom results in breaking six Ti-O bonds, leaving six O dangling bonds and four holes. The distances between the O atoms around the vacancy are too large for the formation of O-O bonds. The resulting holes, instead of being uniformly distributed among all six O atoms, localize on individual O atoms, as in the case of the Sr vacancy. The Ti vacancy can accept up to four electrons, V_{Ti}^{q} with $q = 0, -1, -2, -3, -4$. Figures 5(a) and 5(b) show the structure and spin densities for $q = -2$ and -3; Fig. 5(c) shows the local lattice structure around V_{Ti}^{-4}. The formation energy is shown in Fig. 3(c). The -3 charge state is only metastable, i.e., always higher in energy than -4 and -2 charge states. The transition levels from -4 to -2 occur at 0.81 eV, from -2 to -1 at 0.62 eV, and from -1 to neutral at 0.58 eV above the valence band. Therefore, the Ti vacancy is stable in the -4 charge state in n-type STO, acting as a compensation center.

C. Self-trapped holes

In addition to self-trapped electrons, we also investigated the formation of self-trapped holes. We find that by removing an electron from the valence band of a stoichiometric STO crystal and breaking the local symmetry, the hole left in the valence band becomes localized on an individual O atom, leading to an elongation of the local Ti-O bond length by 4.5%. The spin density of the self-trapped hole is shown in Fig. 2(b), indicating O $2p$ character. The total energy of the supercell containing a self-trapped hole is 0.05 eV lower than that containing a delocalized, free hole at the top of the valence band. This result is not surprising given the low dispersion of the O $2p$–derived valence band in STO, as in other oxides [34]. We conclude that self-trapped holes are stable in STO, at least at low temperatures, in contrast to self-trapped electrons.

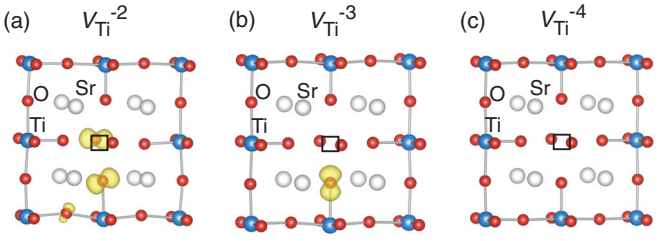

FIG. 5. (Color online) Titanium vacancy in $SrTiO_3$ in different charge states. (a) V_{Ti}^{-2}. (b) V_{Ti}^{-3}. (c) V_{Sr}^{-4}. The vacancy location is indicated with an empty square. The spin densities for V_{Ti}^{-2} and V_{Ti}^{-3} are also shown, with the isosurfaces corresponding to 10% of the maximum.

D. Impact on optical properties

Optical transitions involving defect levels need to be distinguished from thermodynamic transition levels. The Fermi-level positions where formation energies of different charge states cross, in plots such as Fig. 3, correspond to thermodynamic transition levels, in which the defect changes its charge state from q to q' and the atomic positions assume their equilibrium configuration both before and after the transition. Thermodynamic levels can be probed, for example, in deep-level transient spectroscopy (DLTS). In contrast, optical transitions need to be determined using a configuration coordinate diagram. The local lattice relaxations strongly depend on the charge state, leading to significant Stokes shifts and strong vibrational broadening of luminescence peaks. Peak positions can be determined using the Franck-Condon principle, by assuming that the atoms around the defect do not have time to relax during the transition from charge state q to charge state $q' = q \pm 1$, and can thus be obtained from the formation energies in charge states q and q', both in the lattice configuration of the initial charge state q. Optical transition levels are usually determined in photoluminescence (PL) or cathodoluminescence (CL) experiments.

First, we consider the case of an oxygen vacancy in n-type STO. The vacancy is most stable in the (V_O^{+2}+ 1 polaron) configuration [Figs. 1(e) and 1(f)], meaning that an electron in the form of a small polaron is bound to V_O^{+2}. Upon excitation, as in PL or CL experiments, electrons are generated in the conduction band and holes in the valence band. The localized electron near the vacancy can recombine with a hole in the valence band, as depicted in Fig. 6(a), leaving the vacancy in the +2 charge state. The calculated peak emission energy for

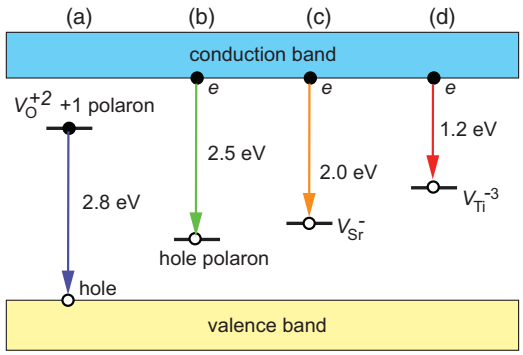

FIG. 6. (Color online) Microscopic mechanisms for luminescence processes in $SrTiO_3$. (a) Recombination of an electron trapped in an oxygen vacancy with a hole in the valence band, resulting in blue luminescence. (b) Recombination of a free electron with a self-trapped hole. (c),(d) Recombination of a free electron with a hole trapped at (c) a Sr vacancy or (d) a Ti vacancy.

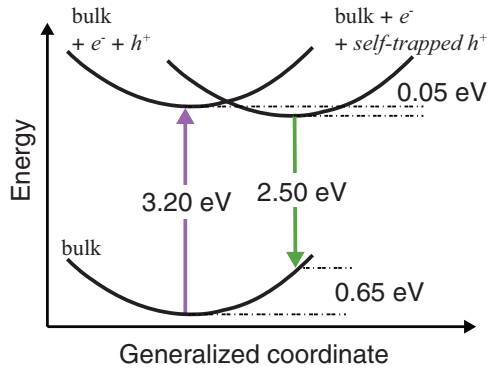

FIG. 7. (Color online) Configuration coordinate diagram for the green luminescence in $SrTiO_3$. An electron-hole pair is created by above-band-gap light excitation. The hole becomes self-trapped, and an electron in the conduction band recombines with the self-trapped hole, resulting in green luminescence.

the process $(V_O^{+2} + 1\text{polaron}) + \text{hole} \rightarrow V_O^{+2}$ is 2.8 eV. This result shows that the oxygen vacancy is responsible for the blue luminescence peak, i.e., 0.4 eV less than the band-gap energy, which is characteristic of a deep level located several tenths of an eV below the band edge. This behavior coexists with the nature of the oxygen vacancy as a shallow donor, which implies a level very close to the band edge. The paradox regarding this dual behavior is thus resolved by considering the fact that two different charge-state transitions are involved for this double donor: the +2/+ transition, which due to the polaronic character of the electron in the + charge state lies well below the conduction band, and the +/0 transition, which has shallow-donor character.

We now turn to the source of the green luminescence. Our results indicated that a self-trapped hole is slightly lower in energy than a free hole in the valence band. We thus expect that, at low temperatures, holes will readily become self-trapped. Upon electron-hole creation, a free electron in the conduction band will find and recombine with a self-trapped hole. This process is illustrated in Fig. 6(b). We find that a free electron recombining with a self-trapped hole leads to an emission peak at 2.5 eV, according to the calculated configuration diagram shown in Fig. 7. This explains the dominance of the green luminescence at low temperatures [9]. As the temperature increases, the concentration of self-trapped holes decreases; indeed, with a 50 meV binding energy, self-trapped holes are easily "ionized" to give rise to free holes in the valence band. The small electron polaron trapped in the oxygen vacancy then recombines with the available free holes, resulting in the blue luminescence of Fig. 6(a). Our calculated hole polaron binding energy of 50 meV can thus be interpreted as an activation energy for the luminescence intensity as a function of temperature. This value is in very good agreement with the activation energy of 43 meV that was determined by fitting the integrated intensity of the green luminescence as a function of temperature [9,11], confirming our proposal for the involvement of hole polarons.

Our results thus explain the shift from green to blue luminescence as a function of temperature [9]. Since self-trapped holes are intrinsic to STO at low temperatures, it also explains why the green luminescence (which does not require the presence of point defects) is observed in undoped and nonirradiated STO samples. The blue luminescence, on the other hand, is expected to increase with the concentration of oxygen vacancies, which can be increased by vacuum annealing or by irradiation [9].

We also considered optical transitions involving Sr or Ti vacancies. For the Sr vacancy, after electron-hole excitations, a hole is captured by the negatively charged vacancy V_{Sr}^{-2}, turning it into V_{Sr}^{-1}. An electron in the conduction band then recombines with the localized hole bound to V_{Sr}^{-1}, returning the Sr vacancy to its original configuration (V_{Sr}^{-2}). We find that this recombination leads to an emission peak at 2.0 eV [Fig. 6(c)]. An analogous process occurs for the Ti vacancy. The vacancy is initially in the V_{Ti}^{-4} configuration. After electron-hole pairs are created, the vacancy traps a hole and turns into V_{Ti}^{-3}. A free electron in the conduction band recombines with the localized hole at V_{Ti}^{-3}, resulting in an emission peak at 1.2 eV, as illustrated in Fig. 6(d). We suggest that the Sr vacancy is responsible for the luminescence peak around 2.0 eV that has been observed [6,13], but the origin of which had not previously been addressed.

Finally, we also investigated the possible formation of a self-trapped exciton, in which a self-trapped hole is next to a self-trapped electron. These calculations were performed by constraining the occupation of the single-particle levels, breaking the symmetry of the lattice, and allowing for lattice relaxations. We find that the self-trapped exciton is unstable, spontaneously relaxing to a configuration with a free electron and a self-trapped hole. Similarly, we find that a self-trapped hole near a ($V_O^{+2} + 1$ polaron) complex is unstable. We attribute these findings to unfavorable strain fields, since both the self-trapped hole and the localized electron (either self-trapped or near the oxygen vacancy) require Ti-O bonds to be elongated. A local expansion of one Ti-O bond tends to favor compression of the next O-Ti bond, making the pairing unstable.

The mechanisms for green and blue luminescence in STO, as described above, are generic in nature and also expected to occur in other complex oxides such as $LiTaO_3$, $LiNbO_3$, $KTaO_3$, and $BaTiO_3$, in which PL peaks are observed that significantly shift between 10 K and room temperature [14]. These compounds are similar to STO, with the transition-metal atoms forming a backbone of corner-sharing octahedra with the O atoms at the vertices, and the *A* site occupied by a highly electropositive atom (Li, K, and Ba). In all of these compounds, oxygen vacancies are expected to bind one or two electrons, and holes to become self-trapped. At low temperature recombination will be dominated by the self-trapped holes, whereas at room temperature recombination will involve electrons bound to the oxygen vacancies and free holes. Our results therefore provide not only a detailed explanation for the experimental observations in STO, but also a comprehensive framework for understanding electronic and optical processes in other complex oxides.

IV. SUMMARY

We have described the intricate relation between vacancies and small polarons in STO. We find that oxygen vacancies are

effectively single donors in *n*-type STO and give rise to blue luminescence, acting simultaneously as a shallow donor and a deep center. Holes, created in excitation processes, become self-trapped at low temperatures, and the recombination of a free electron with a self-trapped hole results in green luminescence. Therefore, at low temperatures, free electrons recombine with self-trapped holes. As the temperature is raised, self-trapped holes become unstable with respect to free holes; electrons bound to the oxygen vacancy then recombine with the free holes giving rise to blue emission, explaining the experimental observations.

ACKNOWLEDGMENTS

This work was supported by the U. S. Army Research Office under Grant No. W911-NF-11-1-0232. M.C. was supported by the ONR Dielectric Enhancements for Innovative Electronics Multidisciplinary University Initiative (Grant No. N00014-10-1-0937). Computational resources were provided by the Center for Scientific Computing at the CNSI, MRL (an NSF MRSEC, DMR-1121053) and NSF CNS-0960316, and by the Extreme Science and Engineering Discovery Environment (XSEDE), supported by NSF ACI-1053575 (TG-DMR070072N).

[1] K. van Benthem and C. Elsässer, J. Appl. Phys. **90**, 6156 (2001).
[2] A. Ohtomo and H. Y. Hwang, Nature (London) **427**, 423 (2004).
[3] P. Moetakef, T. A. Cain, D. G. Ouellette, J. Y. Zhang, D. O. Klenov, A. Janotti, C. G. Van de Walle, S. Rajan, S. J. Allen, and S. Stemmer, Appl. Phys. Lett. **99**, 232116 (2011).
[4] G. Herranz, M. Basletić, M. Bibes, C. Carrétéro, E. Tafra, E. Jacquet, K. Bouzehouane, C. Deranlot, A. Hamzić, J.-M. Broto, A. Barthélémy, and A. Fert, Phys. Rev. Lett. **98**, 216803 (2007).
[5] D. A. Muller, N. Nakagawa, A. Ohtomo, J. L. Grazul, and H. Y. Hwang, Nature (London) **430**, 657 (2004).
[6] S. Mochizuki, F. Fujishiro, and S. Minami, J. Phys.: Condens. Matter **17**, 923 (2005).
[7] D. Kan, T. Terashima, R. Kanda, A. Masuno, K. Tanaka, S. Chu, H. Kan, A. Ishizumi, Y. Kanemitsu, Y. Shimakawa, and M. Takano, Nat. Mater. **4**, 816 (2005).
[8] A. Kalabukhov, R. Gunnarsson, J. Börjesson, E. Olsson, T. Claeson, and D. Winkler, Phys. Rev. B **75**, 121404(R) (2007).
[9] Y. Yamada, H. Yasuda, T. Tayagaki, and Y. Kanemitsu, Phys. Rev. Lett. **102**, 247401 (2009).
[10] R. Leonelli and J. L. Brebner, Phys. Rev. B **33**, 8649 (1986).
[11] T. Hasegawa, M. Shirai, and K. Tanaka, J. Lumin. **87-89**, 1217 (2000).
[12] D. Kan, R. Kanda, Y. Kanemitsu, Y. Shimakawa, M. Takano, T. Terashima, and A. Ishizumi, Appl. Phys. Lett. **88**, 191916 (2006).
[13] A. Rubano, D. Paparo, F. Miletto Granozio, U. Scotti di Uccio, and L. Marrucci, J. Appl. Phys. **106**, 103515 (2009).
[14] Y. Yamada and Y. Kanemitsu, J. Lumin. **133**, 30 (2013).
[15] H. lhrig, J. H. T. Hengst, and M. Klerk, Z. Phys. B **40**, 301 (1981).
[16] J. Zhang, S. Walsh, C. Brooks, D. G. Scholm, and L. J. Brillson, J. Vac. Sci. Technol. B **26**, 1466 (2008).
[17] K.-H. Yang, T.-Y. Chen, N.-J. Ho, and H.-Y. Lu, J. Am. Ceram. Soc. **94**, 1811 (2011).
[18] R. I. Eglitis, E. A. Kotomin, and G. Borstel, Eur. Phys. J. B **27**, 483 (2002).
[19] D. Ricci, G. Bano, G. Pacchioni, and F. Illas, Phys. Rev. B **68**, 224105 (2003).
[20] J. Carrasco, F. Illas, N. Lopez, E. A. Kotomin, Yu. F. Zhukovskii, S. Piskunov, J. Maier, and K. Hermansson, Phys. Status Solidi C **2**, 153 (2005).
[21] V. E. Alexandrov, E. A. Kotomin, J. Maier, and R. A. Evarestov, Eur. Phys. J. B **72**, 53 (2009).
[22] C. Mitra, C. Lin, J. Robertson, and A. A. Demkov, Phys. Rev. B **86**, 155105 (2012).
[23] M. Choi, F. Oba, Y. Kumagai, and I. Tanaka, Adv. Mater. **25**, 86 (2013).
[24] W. Kohn and L. J. Sham, Phys. Rev. **140**, A1133 (1965).
[25] J. Heyd, G. E. Scuseria, and M. Ernzerhof, J. Chem. Phys. **118**, 8207 (2003); **124**, 219906 (2006).
[26] P. E. Blöchl, Phys. Rev. B **50**, 17953 (1994).
[27] G. Kresse and J. Furthmüller, Comput. Mater. Sci. **6**, 15 (1996).
[28] L. Cao, E. Sozontov, and J. Zegenhagen, Phys. Status Solidi A **181**, 387 (2000).
[29] C. Freysoldt, J. Neugebauer, and C. G. Van de Walle, Phys. Rev. Lett. **102**, 016402 (2009).
[30] C. Freysoldt, J. Neugebauer, and C. G. Van de Walle, Phys. Status Solidi B **248**, 1067 (2011).
[31] K. Jacob and G. Rajitha, J. Chem. Thermodyn. **43**, 51 (2011).
[32] M. W. Chase, Jr., *NIST-JANAF Thermochemical Tables*, 4th ed., J. Phys. Chem. Ref. Data (NIST, Washington, DC, 1998), Monograph 9, pp. 1–1951.
[33] A. Janotti, J. B. Varley, P. Rinke, N. Umezawa, G. Kresse, and C. G. Van de Walle, Phys. Rev. B **81**, 085212 (2010).
[34] J. B. Varley, A. Janotti, C. Franchini, and C. G. Van de Walle, Phys. Rev B **85**, 081109(R) (2012).